Photonic Crystals from Core-Shell Colloids with Incorporated Highly Fluorescent Quantum Dots

Friederike Fleischhaker and Rudolf Zentel*

Institute of Organic Chemistry, Department of Chemistry and Pharmacy, University of Mainz, Duesbergweg 10-14, 55128 Mainz, Germany

Received October 29, 2004. Revised Manuscript Received December 21, 2004

We report the preparation of nanoscaled PS/PMMA core-shell spheres with highly fluorescent CdS/ZnS coated CdSe quantum dots (QDs) integrated in the core. Core-shell spheres of different diameters have been self-assembled to colloidal photonic crystals (PCs) with photonic stop bands located in the visible range of the electromagnetic spectrum. For the synthesis of the core, a modified miniemulsion polymerization has been used; the shell was prepared by a newly developed core-shell polymerization. The CdSe QDs embedded in the core were coated with the higher band gap semiconductor materials CdS and ZnS in a successive ion layer adsorption reaction (SILAR) keeping up the light-emitting properties of the QDs during the integration process. A modifying influence of the photonic band structure of the PC on the photoluminescence (PL) of the embedded QDs was observed by angular-dependent fluorescence measurements. The controlled combination of electronic confinement, originating from the QDs, and photon confinement, due to the periodic dielectric structure of the colloidal crystal, as it has been realized in this work presents a huge platform for the design and construction of novel optoelectronic devices based on PCs.

Introduction

Photonic crystals (PCs) are a fascinating class of materials and highly promising candidates for a variety of nanoscaled optoelectronic devices.[1,2] They are generally characterized by a periodic dielectric structure that induces the opening of photonic stop bands or band gaps due to Bragg diffraction, in which the photon density of states can be depleted. Consequently, in these particular wavelength ranges that are at the PCs' lattice vector scale, the propagation of electromagnetic radiation is blocked entirely or at least in certain lattice directions.[3] This property can be exploited to modify the spontaneous emission of light sources incorporated into the PC such as organic dyes,[4−9] rare earth ions,[8,10] or semiconductor quantum dots (QDs).[8,11−14] Colloidal PCs that are also known as artificial opals are important representatives of 3D PCs with stop bands in the visible or NIR wavelength range. They are self-assembled from monodisperse nanospheres made of polymers or SiO_2 by bottom-up methods and can be fabricated at low cost and large scale, required by mass production.[15−17]

Semiconductor QDs with diameters in the lower nanometer range (1−10 nm) exhibit size-tunable electronic and optical properties because of 3D electronic confinement.[18] By doping PCs with fluorescent QDs, discrete electronic and photonic states can be combined as well as separately engineered within a single structure. This presents a powerful platform for the creation of novel nanoscaled light sources with controllable spontaneous emission.

Up to now, semiconductor QDs have been incorporated into the voids of colloidal crystals either by in-situ growth methods (such as chemical vapor and chemical or electrochemical bath deposition)[11−13] or by electrostatic fixation on the surface of polymer spheres being subsequently crystallized to artificial opals.[14] Additionally, "raisin bun"-type SiO_2 spheres with semiconductor QDs have been prepared by a multistep silanization process.[19] However, incorporation of QDs into the voids of colloidal crystals does not protect the QDs from oxidation. Furthermore, the mentioned in-situ

---

* Author to whom correspondence should be addressed. E-mail: zentel@uni-mainz.de; phone: (+49) 6131−39−20361.

(1) Yablonovitch, E. *Phys. Rev. Lett.* **1987**, *58*, 2059.
(2) John, S. *Phys. Rev. Lett.* **1987**, *58*, 2086.
(3) Joannopoulos, J. D.; Meade, R. D.; Winn, J. N. *Photonic Crystals, Molding the Flow of Light*; Princeton University Press: Singapore, 1997.
(4) Müller, M.; Zentel, R.; Maka, T.; Romanov, S. G.; Sotomayor Torres, C. M. *Chem. Mater.* **2000**, *12*, 1499.
(5) Romanov, S. G.; Maka, T.; Sotomayor Torres, C. M.; Müller, M.; Zentel, R. *Appl. Phys. Lett.* **1999**, *75*, 1057.
(6) Romanov, S. G.; Maka, T.; Sotomayor Torres, C. M.; Müller, M.; Zentel, R. *J. Appl. Phys.* **2002**, *91*, 9426.
(7) Romanov, S. G.; Maka, T.; Sotomayor Torres, C. M.; Müller, M.; Zentel, R. *Appl. Phys. Lett.* **2001**, *79*, 731.
(8) Gaponenko, S. V.; Bogomolov, V. N.; Petrov, E. P.; Kapitonov, A. M.; Yarotsky, D. A.; Kalosha, I. I.; Eychmüller, A. A.; Rogach, A. L.; McGilp, J.; Woggon, U.; Gindele, F. *J. Lightwave Technol.* **1999**, *17*, 2128.
(9) Megens, M.; Wijnhoven, J. E. G. J.; Lagendijk, A.; Vos, W. L. *J. Opt. Soc. Am. B* **1999**, *16*, 1403.
(10) Kalkman, J.; de Bres, E.; Polman, A.; Jan, Y.; Norris, D. J.; 't Hart, D. C.; Hoogenboom, J. P.; van Blaaderen, A. *J. Appl. Phys.* **2004**, *95*, 2297.
(11) Blanco, A.; Lopez, C.; Mayoral, R.; Miguez, H.; Meseguer, F.; Mifsud, A.; Herrero, J. *Appl. Phys. Lett.* **1998**, *73*, 1781.
(12) Vlasov, Y. A.; Luterova, K.; Pelant, I.; Hönerlage, B.; Astratov, V. N. *Thin Solid Films* **1998**, *318*, 93.
(13) Romanov, S. G.; Folkin, A. V.; Alperovich, V. I.; Johnson, N. P.; de la Rue, R. M. *Phys. Status Solidi A* **1997**, *164*, 169.
(14) Wang, D.; Rogach, A. L.; Caruso, F. *Chem. Mater.* **2003**, *15*, 2724.
(15) Egen, M.; Zentel, R. *Chem. Mater.* **2002**, *14*, 2176.
(16) Wong, S.; Kitaev, V.; Ozin, G. A. *J. Am. Chem. Soc.* **2003**, *125*, 15589.
(17) Reese, C. E.; Guerrero, C. D.; Weissman, J. M.; Lee, K.; Asher, S. A. *J. Colloid. Interface Sci.* **2000**, *232*, 76.
(18) Alivisatos, A. P. *Science* **1996**, *277*, 933.
(19) Rogach, A. L.; Nagesha, D.; Ostrander, J. W.; Giersing, M.; Kotov, N. A. *Chem. Mater.* **2000**, *12*, 2676.

10.1021/cm0481022 CCC: $30.25

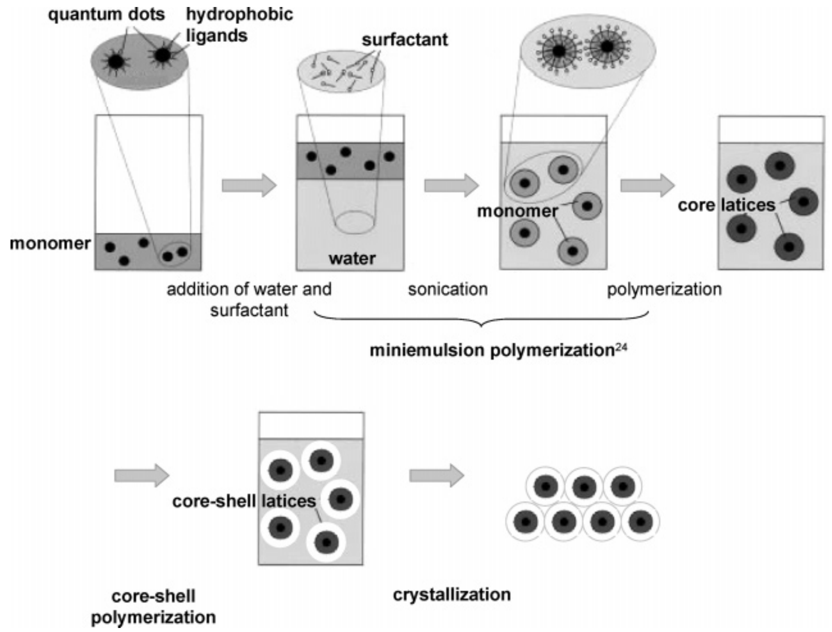

Figure 1. Schematic illustration of QD incorporation into the core of core-shell colloids.

growth methods[11−13] do not allow the formation of high-quality QDs known for low polydispersity and strong photoluminescence (PL). The electrostatic fixation of QDs on the surface of polymer spheres requires QDs surrounded by hydrophilic ligands such as thioglycolic acid[14] that are well-known PL reducing agents.[20] Concerning PCs from “raisin bun”-type SiO_2 spheres doped with QDs, no significant PL is obtained.[19]

In this work, we report the synthesis of composite PCs from polymer core-shell spheres with incorporated highly fluorescent monodisperse CdSe QDs in the core. Furthermore, the influence of the photonic band structure on the PL of the embedded QDs is successfully investigated.

Experimental Section

(a) Synthesis of CdS/ZnS Coated CdSe QDs. The synthesis of the uncoated CdSe QDs was done according to standard procedures.[21]

The SILAR coating was performed by modifying the reaction procedure reported by Peng et al.[22] Additionally to the cadmium and sulfur injection solutions a zinc solution was prepared by dissolving 0.485 g ZnO in 10.83 g oleic acid and 108 mL octadecene at 250 °C under argon flow. After a clear solution had been obtained, it was cooled to 60 °C. The zinc injection solution was used to prepare a SILAR coating consisting of three layers of CdS and three additional layers of ZnS. The synthesis of the ZnS layers was carried out in analogy to that of the CdS layers.

(b) Synthesis of PS Core Colloids with Incorporated CdS/ZnS Coated CdSe QDs. 2.39×10^{-6} mmol of CdS/ZnS coated CdSe QDs was dispersed in 0.33 g styrene and 0.014 g hexadecane. A solution of 0.014 g sodium dodecyl sulfate (SDS) dissolved in 1.34 g deionized water was added and the mixture was stirred for 1 h. The miniemulsion was prepared by ultrasonifying the emulsion for 150 s with a Branson Sonifier W250 Digital (amplitude: 70%) supplied with a conical standard microtip. The polymerization was started with 0.01 g potassium persulfate at a temperature of 70 °C and was completed in less than 2 h.

(c) Synthesis of PS/PMMA Core-Shell Colloids with Incorporated CdS/ZnS Coated CdSe QDs in the Core. 0.6−0.8 mL of the dispersion prepared in (b) were diluted with 45 mL deionized water and flooded with nitrogen for 30 min. Subsequently, 0.05 g AIBN dissolved in 0.3 mL MMA was added and the mixture was heated to 70 °C. Next, MMA was continuously injected at a speed of 6 mL/h. The size of the core-shell colloids could be controlled by the injected volume of MMA as well as by the amount of core particles used in this reaction (eq 1). When the desired size of the colloids was obtained, the injection of MMA was stopped. Having stirred the mixture for a further 5 min, the reaction was quenched with air and filtered afterwards to remove minor traces of agglomerates.

(d) Crystallization of the Core-Shell Spheres to Colloidal Crystals. The crystallization of the core-shell spheres to artificial opals was performed according to the same procedure we already reported for other types of polymer spheres.[23]

(e) Instrumental Details. Transmission electron microscopy was carried out using a FEI Tecnai F30 TEM. UV/vis absorption spectra were recorded on a Shimadzu UV-2102 PC spectrometer. PL spectra were taken with a FluoroMax-2 spectrometer from ISA JOBIN YVON-SPEX Instruments S. A. The PL in the angular-dependent fluorescence measurements was excited by a Spectra Physics Beam Lock 2080 cw argon ion laser at 457.9 nm. The photographs were taken with a Kodak digital camera DX 3900.

Results and Discussion

The synthesis of core-shell colloids with embedded CdSe QDs in the core was performed according to the following procedure (Figure 1): Initially, highly fluorescent CdSe QDs that are resistant to the required chemical and mechanical treatment were synthesized. Then, monodisperse core colloids were prepared by a modified miniemulsion process[24] that

---

(20) Potapova, I.; Mruk, R.; Prehl, S.; Zentel, R.; Basché, T.; Mews, A. *J. Am. Chem. Soc.* **2003**, *125*, 320.

(21) Qu, L.; Peng, X. *J. Am. Chem. Soc.* **2002**, *124*, 2049.

(22) Li, J., J.; Wang, Y. W.; Guo, W.; Keay, J. C.; Mishima, T. D.; Johnson, M. B.; Peng, X. *J. Am. Chem. Soc.* **2003**, *125*, 12567.

(23) Egen, M.; Voss, R.; Griesebock, B.; Zentel, R. *Chem. Mater.* **2003**, *15*, 3786.

(24) Landfester, K. *Macromol. Rapid Commun.* **2001**, *22*, 896.

allowed the incorporation of fluorescent QDs. Finally, the core particles were converted into core-shell colloids by a newly developed core-shell polymerization technique and crystallized to opals with photonic stop bands located in the visible range of the electromagnetic spectrum.

CdSe QDs. CdSe QDs with hydrophobic ligands (hexadecylamine) were prepared according to Peng et al. in a molecular precursor route.[21] To passivate surface nonradiative recombination sites reducing fluorescence quantum yields, the particles were coated with the higher band gap semiconductor materials CdS and ZnS using a modified SILAR reaction.[22] QDs prepared by this method showed strong fluorescence even after having been subjected to the miniemulsion and core-shell polymerization process. That is probably due to a uniform and complete coverage of the CdSe surface resulting from a layer-by-layer coating and a smooth adaptation of the lattice constants from CdSe via CdS to ZnS leading to a mechanically stable and fluorescence protecting coating.

However, CdSe QDs that were only coated with ZnS using a different method reported by Bawendi et al.[25] failed to show fluorescence after incorporation into core-shell spheres. We assume that this observation is due to a mechanically less stable and less uniform ZnS shell. Reasons for this are probably the abrupt lattice constant change from CdSe to ZnS as well as the formation of islandlike ZnS clusters on the CdSe surface. These clusters finally coalesce and lead to grain boundaries within the coating.[25]

Core Colloids. A modified miniemulsion polymerization was used to prepare the core of the core-shell colloids with embedded QDs. The basics of miniemulsions are described elsewhere.[24] A characteristic feature of miniemulsions is that polymerization proceeds in the monomer droplets in contrast to conventional emulsion polymerizations where the micelles are the center of polymerization. Consequently, no diffusion of monomer from monomer droplets through the aqueous phase into the micelles is necessary and nanoparticles dispersed in the monomer phase or rather in the monomer droplets after sonication should be directly integrated into the resulting polymer spheres.

By dispersing a definite amount of SILAR coated CdSe QDs in styrene and subsequently carrying out a miniemulsion process with SDS as surfactant, hexadecane as hydrophobe, and potassium persulfate as initiator, highly fluorescent and monodisperse core colloids doped with QDs could be prepared (Figure 2). According to TEM measurements, the diameter of the cores is about 75 nm. The observed attachment of the spheres at the connecting points (Figure 2A) is caused by the TEM electron beam. Due to the higher electron contrast, the CdSe QDs are visible as small black dots in TEM (Figure 2A). The high-resolution TEM image (Figure 2B) clearly shows the resolved lattice planes of a single SILAR-coated CdSe QD. Besides that, distinct signals for Cd, Se, S, and Zn resulting from the CdSe QDs coated with a CdS/ZnS shell were observed when analyzing the core colloids with EDX. The PL spectrum of an aqueous core colloid dispersion (Figure 2C) shows a pronounced and very narrow luminescence peak. The observed full width at half-maximum of about 30 nm underlines the high monodispersity of the SILAR coated CdSe QDs. Due to strong scattering effects of the dispersion, exact data of quantum yields could not be determined.

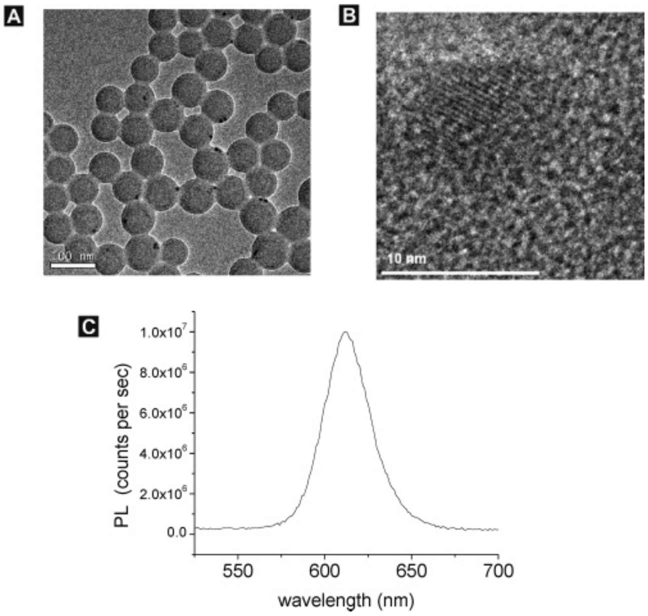

Figure 2. (A) PS core colloids with SILAR-coated CdSe QDs (TEM). The colloid mean diameter is 75 nm with a standard deviation of 6%. The observed attachment of the spheres at the connecting points is due to the TEM electron beam. (B) Single SILAR-coated CdSe QD in high resolution. (C) Fluorescence spectrum of an aqueous core colloid dispersion with SILAR-coated CdSe QDs. The sample was excited at $\lambda = 360$ nm.

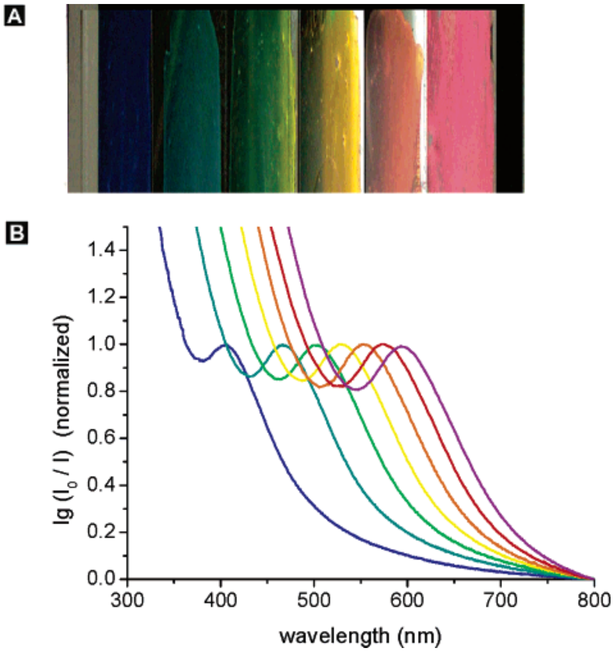

Figure 3. (A) Photograph of colloidal PCs from PS/PMMA core-shell spheres with embedded CdSe QDs. The colors result from the corresponding wavelengths reflected by the opaline structure due to stop bands parallel to the [111] axis of the opal. Varying the size of the spheres allows a shift of the stop bands along the visible range of the electromagnetic spectrum. (B) UV−vis spectra in absorption of the PCs described in A. The spectra were recorded with an angle of incidence parallel to the [111] axis of the crystal. I_0 is the intensity of the incident, and I is the intensity of the transmitted light beam. The peaks are due to stop bands parallel to the [111] axis of the colloidal crystals.

---

(25) Dabbousi, B. O.; Rodriguez-Viejo, J.; Mikulec, F. V.; Heine, J. R.; Mattoussi, H.; Ober, R.; Jensen, K. F.; Bawendi, M. G. *J. Phys. Chem. B* **1997**, *101*, 9463.

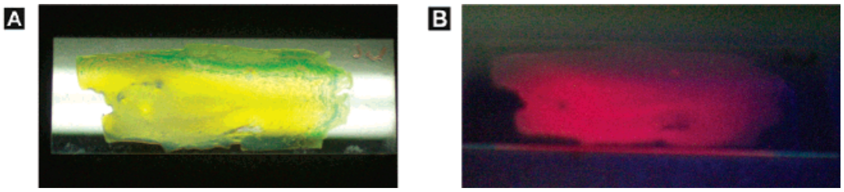

Figure 4. PC from PS/PMMA core-shell colloids with embedded SILAR coated CdSe QDs (photographs). **(A)** The sample is irradiated with white light. The color results from reflected light ($\lambda = 558$ nm) because of the colloidal crystal stop band. **(B)** The sample is irradiated with UV light. The color is caused by the PL of the embedded CdSe QDs ($\lambda_{PL} = 613$ nm).

Styrene presents an excellent monomer for miniemulsions because of its pronounced hydrophobicity and radical polymerizability. Additionally, it is a suitable dispersion agent for CdSe QDs without fluorescence-quenching properties. The amount of CdSe QDs was chosen in a way that each core sphere contains one QD on average. Because of statistical reasons, the exact number of QDs per core as well as the exact location of the QDs could not be controlled. Regarding the QDs in Figure 2A, a driving force to the surface of the PS spheres can be observed. This might result from favorable interactions between the alkyl chains of the hexadecylamine ligands surrounding the QDs and the surfactant SDS used in the miniemulsion process. After the formation of core-shell spheres, the location of the QDs is limited to the core.

Core-Shell Colloids. The preparation of core-shell colloids that are used as fluorescent building blocks for colloidal PCs was performed according to the following considerations:

To prevent the formation of new spheres in addition to (or instead of) the formation of core-shell spheres in this step, any separate generation of monomer droplets as well as any start of the polymerization outside the core spheres should be avoided. Consequently, an oil-soluble initiator was used because of its affinity to the hydrophobic core where it is to start the polymerization. Additionally, the amount of monomer necessary for the synthesis of the shell was added continuously to the core spheres and not en bloc. The speed of monomer addition was adjusted such that the added monomer could be picked up by the core spheres but no separate monomer droplets were formed. PMMA was chosen as material for the shell: MMA presents a suitable monomer for radical polymerization as well as for continuous injection since thermally induced polymerization is unlikely. Because of its hydrophobicity and minimal water solubility, it should be picked up by the polystyrene cores dispersed in water after having been injected.

This newly developed core-shell polymerization allowed the conversion of CdSe doped core particles prepared by miniemulsion into core-shell colloids of controllable size that self-assemble to PCs with stop bands covering the visible range of the electromagnetic spectrum (Figure 3).

Core-shell colloids synthesized according to this procedure and subsequently crystallized to opals showed strong PL due to the embedded CdSe QDs in the core as well as the color of those wavelengths being reflected due to the photonic band structure of the opal (Figure 4).

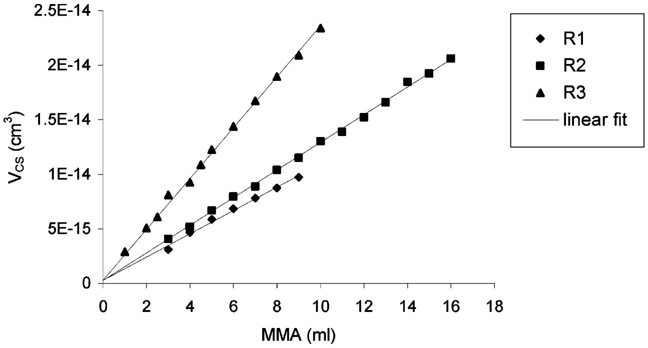

Figure 5. The volume of the core-shell colloids (V_{CS}) synthesized in the core-shell polymerizations (R1, R2, R3) is plotted versus the injected volume of MMA and linear fits are applied. V_{CS} is determined with the help of the Bragg equation[27] and the stop bands of the corresponding opals observed by UV−vis spectroscopy.

Table 1. Characteristic Data of the Core-Shell Polymerizations (R1, R2, R3) Taken from Figure 5[a]

	R1	R2	R3
slope (10^{-15})	1.02	1.27	2.33
intersection (10^{-16} cm^3)	2.74	2.53	2.67
d_{calc} (nm)	81	78	80
d_{TEM} (nm)	75	75	75
N (10^{14})	7.38	6.22	3.39
V_{disp} (mL)	0.8	0.7	0.4

[a] Slopes and intersections of the linear fits, the diameter of the core colloids calculated from the intersections (d_{calc}) and determined from TEM-measurements (d_{TEM}), the amount of core colloids (N) calculated from the slopes, and the volume of core colloid dispersion actually used (V_{disp}).

The size of the core-shell colloids and consequently the photonic stop band position of the opal could be controlled by the amount of core colloids used in the core-shell polymerization as well as by the injected volume of MMA according to the following equation:

$$V_{CS} = V_C + \frac{\rho_{MMA}}{\rho_{PMMA}} \cdot \frac{1}{N} \cdot V_{MMA} \tag{1}$$

Here, V_{CS} is the volume of the core-shell colloids, V_C is the volume of the core colloids, and V_{MMA} is the volume of MMA added to the amount of cores N in the core-shell polymerization. The quotient ρ_{MMA}/ρ_{PMMA} considers the change in density from MMA to PMMA.

Plotting V_{CS} versus V_{MMA} (Figure 5) for different amounts of core colloids of the same diameter used in three different reactions (R1, R2, R3) leads to a graph with pronounced linearity underlining the validity of eq 1. The values for the core colloid diameter (d_{calc}) calculated from the intersections of the linear fits are in good agreement with the diameter (d_{TEM}) according to TEM-measurements, and also the ratios of the core colloid amounts (N) calculated from the slopes perfectly agree with the amounts of core latex dispersion (V_{disp}) used in the core-shell polymerization (Table 1). In general, core-shell spheres with diameters from 150 to

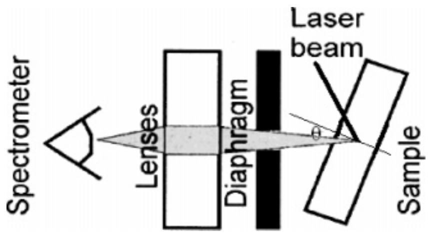

Figure 6. Experimental setup for angular-dependent PL measurements in reflection.

350 nm could be prepared by this procedure. For the preparation of larger spheres, an additional amount of surfactant had to be added during the core-shell polymerization to prevent coalescence of the spheres.

PL Measurements. The effect of the colloidal crystal photonic stop band on the PL of the integrated QDs was investigated by angular-dependent fluorescence measurements. The measurements were performed in reflection and the PL was excited with an argon ion laser at 457.9 nm. The used experimental setup is sketched in Figure 6. In Figures 7B and 7D the normalized intensity of the PL maximum of the CdSe QDs embedded in the core-shell spheres of the investigated opals is plotted versus different angles of detection θ. The angle of detection describes the angle between the emitted light beam and the [111] axis of the colloidal crystal. Since independent of the existence of a photonic band structure, an intensity decrease of the emitted light with increasing angle of detection according to

$$I(\theta) = I(\theta = 0)\cdot\cos\theta \text{ (Lambert law)}^{26} \qquad (2)$$

has to be taken into account, cos (θ) in dependence of θ is plotted as a theoretical reference curve. To reproduce the Lambert law for a nonopal surface, the normalized intensity of the PL maximum of CdSe QDs randomly dispersed in a thin PS film is shown at different angles of detection, too (experimental reference curve). At larger angles θ, the decrease of PL is more enhanced than expected according

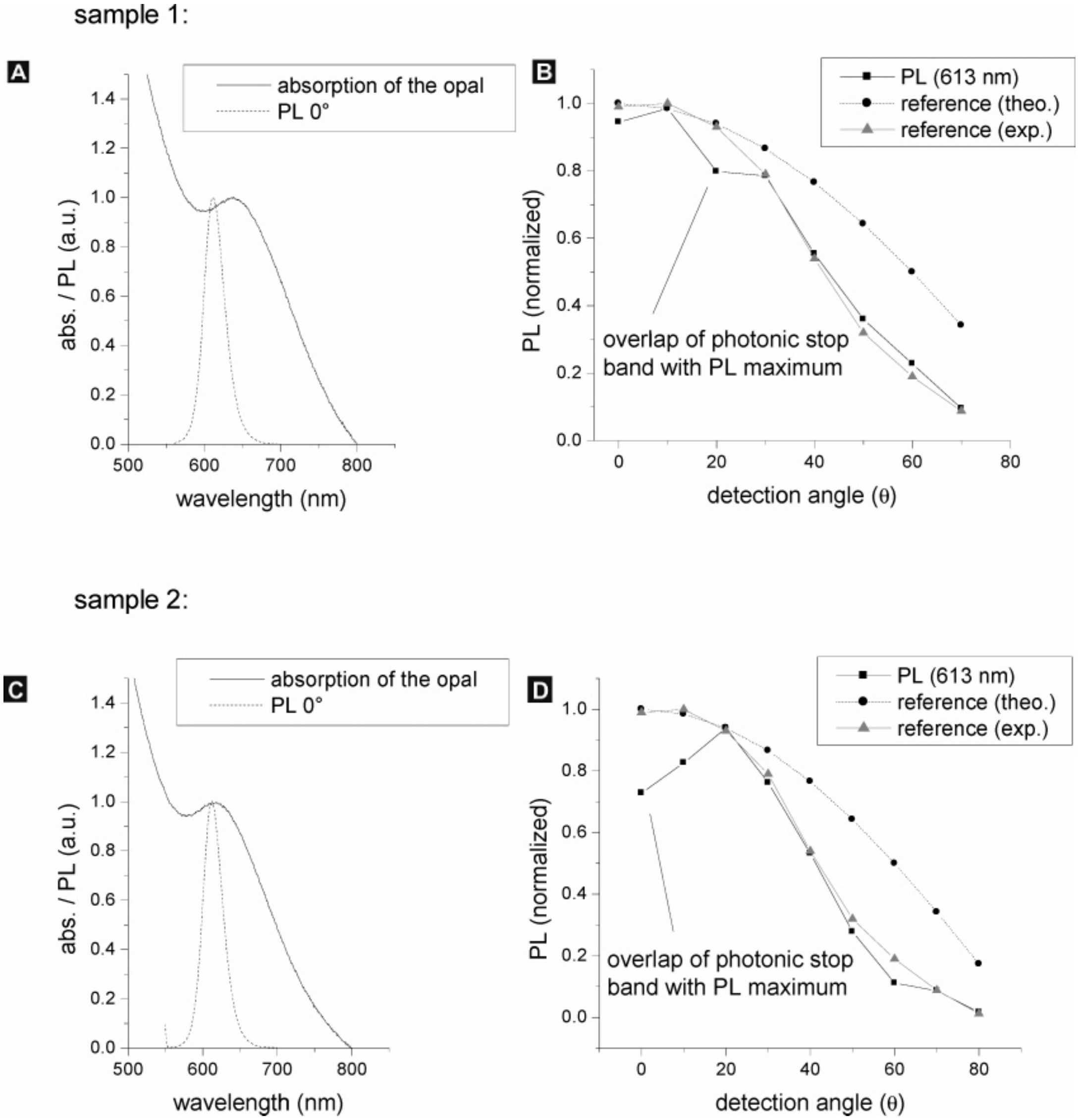

Figure 7. (A, C) Solid line: UV−vis spectra in absorption of colloidal crystals from PS/PMMA core-shell spheres with embedded CdSe QDs. The photonic stop bands along the [111] axis are at $\lambda = 640$ nm (A) and at $\lambda = 614$ nm (C). Dashed line: PL spectra in transmission recorded at $\theta = 0°$. The PL maxima are at $\lambda = 613$ nm. The excitation wavelength is at $\lambda = 457.9$ nm. (B, D) Black solid line: Normalized intensities of the PL maximum of CdSe QDs embedded in the corresponding core-shell colloidal crystals in dependence of the detection angle θ. Black dashed line: Cos θ in dependence of θ (theoretical reference curve). Gray solid line: Normalized intensities of the PL maximum of CdSe QDs randomly dispersed in a nonopal PS film (experimental reference curve).

to the Lambert law, which is probably due to a slight photodegradation of the CdSe QDs during the measurements.

The PL maximum of the CdSe QDs is at $\lambda_{PL} = 613$ nm, and the photonic stop bands parallel to the [111] axis of the investigated colloidal crystals are at $\lambda = 640$ nm and $\lambda = 614$ nm (Figures 7A and 7C). According to the Bragg law,[27] the stop bands of colloidal PCs are shifted to smaller wavelengths with increasing angle θ. In Figures 7B and 7D, a reduction of the PL intensity can be observed at those angles θ that allow the stop bands of the colloidal crystals to overlap with the fluorescence maximum of the embedded QDs. The measurements are reproducible and measurement errors concerning the PL intensity are limited to maximal 5% for detection angles between 0 and 50°. Despite the fact that light emitted by QDs close to the surface of the colloidal crystal and an imperfect lattice structure limit the PL reduction to 25%, a modifying effect of the photonic band structure on the spontaneous emission of the QDs could be shown.

Acknowledgment. Financial support from the DFG (Schwerpunkt: Photonische Kristalle) is highly appreciated. Thanks are due to Prof. Th. Basché, Prof. A. Mews, Dr. I. Potapova, and R. Xie (University of Mainz) for helpful discussions and the introduction into the field of QDs. Thanks are also due to Dr. S. Romanov (University of Wuppertal) for the introduction into angular-dependent PL measurements.

CM0481022

---

(26) Vogel, H. *Gerthsen Physik*; Springer: Berlin, 1999.

(27) $\lambda = 2\,(^2/_3)^{1/2} d(n^2 - \sin^2(\theta))^{1/2}$, where λ is the wavelength of the stop bands of the colloidal crystal, d is the diameter of the spheres, n is the effective refractive index, and θ is the angle between the light beam and the [111] axis of the colloidal crystal. See, for example: Flaugh, P. L.; O'Donnell, S. E.; Asher, S. A. *Appl. Spectrosc.* **1984**, *38*, 847.